Generation of acoustic and optical vortices in the course of mechanical bending and collinear acousto-optic diffraction

Mys O., Kostyrko M., Adamenko D., Skab I. and Vlokh R.

O. G. Vlokh Institute of Physical Optics, 23 Dragomanov Street, 79005 Lviv, Ukraine. e-mail: vlokh@ifo.lviv.ua

Abstract. We show that a bending mechanical stress can produce a topological defect of orientation of the eigenvectors of Christoffel tensor with the strength equal to ½. This implies generation of a singly charged acoustic vortex for transverse acoustic waves. In general, this vortex is anisotropic, although it can be transformed into isotropic one at some geometrical parameters of distributed mechanical load. The acoustic vortices generated by the bending stresses can be produced even in isotropic solid-state media. Using the example of crystals belonging to the point symmetry group 3m, we also consider the process of backward collinear acousto-optic diffraction for the case of interactions of optical and acoustic waves that bear bending-generated topological defects of their phase fronts. It is demonstrated that, in the case of linearly polarized incident optical wave, a vector beam with a unit polarization order is generated in the crystals. Acousto-optic interaction of this vector beam with the acoustic beam bearing a singly charged anisotropic vortex produces a diffracted optical wave that bears a vortex, too. The embedded topological defect of the phase front associated with this vortex has the strength given by a sum of strengths of the topological defects of the incident optical wave and the acoustic wave. The diffracted optical beam represents an anisotropic vortex beam with the orbital angular momentum (OAM) equal to $2\hbar$. When both the acoustic wave and the incident optical wave nest the bending-induced singly charged anisotropic vortices, the diffracted optical wave would also bear a vortex. Its charge is a linear combination of the charges referred to the acoustic and incident optical waves, which involves the parameters of acoustic and optical anisotropies. When the signs of OAMs of the interacting acoustic and optical waves are the same, the diffracted optical wave bears a doubly charged anisotropic optical vortex. At some specific anisotropy parameters, it can be transformed into isotropic vortex. Finally, the topological defects embedded in the interacting waves annihilate and the diffracted optical wave becomes vortex-free when the signs of OAMs of the interacting waves are opposite.

Keywords: acoustic vortices, bending stresses, acousto-optic diffraction

UDC: 535.012+534.2

1. Introduction

In our recent work [1] we have shown that mechanical torsion stresses can impose acoustic singularities of the eigenvectors of Christoffel tensor due to a piezo-acoustic effect [2, 3]. This produces a singly charged acoustic vortex beam propagating inside a crystal. We have also demonstrated that the process of backward collinear acousto-optic (AO) interaction of a linearly polarized incident optical wave with a torsion-induced acoustic vortex wave in crystals is accompanied by generation of a vector beam with a unit polarization order. AO interaction of this vector beam with the acoustic beam bearing a singly charged vortex results in a vortex-bearing

diffracted optical wave. It has an embedded topological defect of its phase front, the strength of which is given by the sum of strengths of topological defects of the incident optical wave and the acoustic wave (AW). Then the diffracted optical beam would also bear a vortex with the orbital angular momentum (OAM) equal to $2\hbar$ [4]. If the torsion-induced circular optical vortex wave interacts with the acoustic vortex wave of the same chirality, the diffracted optical wave would bear a doubly charged vortex. In the case of AO interaction of the waves with the opposite chiralities and the vortices having the opposite signs of their charges, the latter vortices would annihilate in the process of AO diffraction so that the diffracted optical wave becomes vortex-free.

Notice that the effects described above can occur in the crystals that belong to the point symmetry groups 3m, 32, $\overline{3}m$, 3, $\overline{3}$, 23, m3, 432, $\overline{4}3m$ and m3m, provided that the torsion moment is applied along the three-fold symmetry axis. This limits the kinds of material media where the effect can be observed to the crystals having one or more three-fold axes among their symmetry elements. On the other hand, we have shown [6] that mechanical bending of solid-state media can also produce polarization singularities nested in optical beams and corresponding singly charged optical vortices. In general, these vortices are anisotropic [6], i.e. the relevant optical field contains a mixed screw-edge dislocation of its phase front [7]. At some values of geometric parameters, the vortex can be transformed into isotropic one.

Maybe, the most important characteristic of this method of generation of optical vortices is that bending stresses can induce polarization singularities in the crystals of arbitrary symmetries and even in isotropic glasses. In the present work, we analyze the possibilities for generation of acoustic polarization singularities and acoustic vortices through application of mechanical bending to glass-like media. The other subject of this work is a potential transfer of acoustic OAM from acoustic to optical beams, which takes place in the course of AO diffraction in crystals.

2. Method of analysis

Let us consider a parallelepiped-shaped optical sample prepared from BK7 glass. The latter is characterized by the refractive index $n = 1.52$ [8] and the piezo-optic coefficient $\langle\pi_{66}\rangle = \langle\pi_{11}\rangle - \langle\pi_{12}\rangle = -1.591\times10^{-12}$ m^2/N [9] at the wavelength $\lambda = 632.8$ nm of optical radiation. The sizes of the beam-like glass sample are taken to be $b = 3.0$ mm, $h = 3.22$ mm and $l = 16.0$ mm.
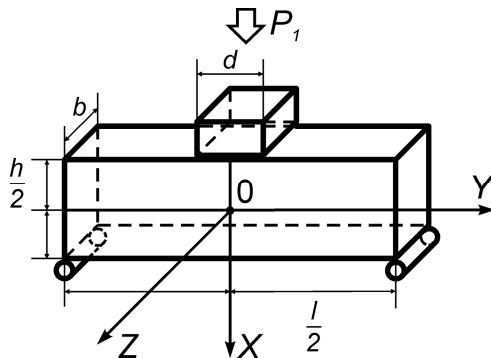
Fig. 1. Scheme of application of mechanical load distributed over distance d on an upper sample surface.

Let a distributed load $P_1 = 20.0$ N be applied along the X axis (see Fig. 1). Suppose that a glass beam is placed on two cylindrical rods, with the distance between the rods being equal to 16.0 mm. Let the load distributed over the distance d on the upper surface be applied to the glass beam (see Fig. 1) and the optical and acoustic waves propagate along the Z axis. Then we have in the region $-d/2 < Y < d/2$ (see Refs. [10, 11] for more details):

Ukr. J. Phys. Opt. 2022, Volume 23, Issue 3

167

$$Q = \frac{P_1}{2}, \; M = \frac{P_1}{2}\left(\frac{l}{2}+Y\right), \tag{1}$$

where M is the bending moment and Q the transverse mechanical force. The corresponding stress components read as

$$\sigma_2 = \frac{M}{J_Z}X = \frac{6P_1}{bh^3}\frac{d(2l-d)-4Y^2}{4d}X, \tag{2}$$

$$\sigma_6 = \frac{Q}{2J_Z}\left(\frac{h^2}{4}-X\right) = -\frac{6P_1Y}{bh^3d}\left(\frac{h^2}{4}-X^2\right), \tag{3}$$

while the optical-indicatrix rotation angle and the optical birefringence are given by

$$\tan 2\zeta_Z^o = \frac{2\left(h^2/4 - X^2\right)Y}{\left(d(2l-d)/4 - Y^2\right)X} = \frac{2\left(h^2/4 - r^2\cos^2\varphi\right)}{\left(d(2l-d)/4 - r^2\sin^2\varphi\right)}\tan\varphi, \tag{4}$$

$$\Delta n_{12} = \frac{3n^3 P_1}{bh^3 d_o}\pi_{66}\sqrt{\left(\frac{d(2l-d)}{4}-Y^2\right)^2 X^2 + 4\left(\frac{h^2}{4}-X^2\right)^2 Y^2}. \tag{5}$$

At the polar coordinate $r \to 0$, Eq. (4) reduces to

$$\tan 2\zeta_Z^o = -\frac{2\sigma_6}{\sigma_2} = \frac{2h^2}{d(2l-d)}\tan\varphi \tag{6}$$

The above dependence of the angle ζ_Z^o on the azimuthal angle φ corresponds to a so-called anisotropic vortex that appears due to a mixed screw-edge dislocation of the phase front. Under the condition $2h^2/d_o(2l-d_o)=1$ (or $d_o = l - \sqrt{l^2 - 2h^2} \simeq h^2/l$ at $2h^2 \ll l^2$), Eq. (6) yields in

$$\tan 2\zeta_Z^o = \tan\varphi \;\; (\text{or } \zeta_Z^o = \varphi/2), \tag{7}$$

i.e. we deal with a pure screw dislocation of the phase front. It gives rise to the isotropic vortex having the unit charge. Here the notation d_o is introduced to indicate the distance at which the pure screw dislocation of the optical wavefront is achieved. Under the same conditions, the spatial distribution of optical birefringence is given by a conical surface:

$$\Delta n_{12} = \frac{3n^3 P_1 l}{2bh^3}\pi_{66}\sqrt{X^2 + Y^2}. \tag{8}$$

The Young and Poisson coefficients for the BK7 glass are equal respectively to $E = 82.0\,\text{GPa}$ and $\nu = 0.206$ [12], and the density amounts to $\rho = 2510\,\text{kg/m}^3$ [13]. The appropriate elastic-stiffness coefficients can be calculated using the well-known relations

$$C_{12} = \frac{\nu E}{(1-2\nu)(1+\nu)}, \; C_{11} = C_{12} + \frac{E}{1+\nu}. \tag{9}$$

They are equal to $C_{11} = 91.81\,\text{GPa}$ and $C_{12} = 23.82\,\text{GPa}$. Finally, the AW velocities v_{mn} (with the indices m and n corresponding respectively to the directions of propagation and polarization of the AW) can be found from the elastic-stiffness coefficients via the Christoffel equation:

$$C_{ijkl}m_j m_k p_l = \rho v_{mn}^2 p_i. \tag{10}$$

Here C_{ijkl} is the elastic-stiffness tensor written in tensor notation, m_j and m_k imply the unit wavevectors of AWs, and p_l and p_i the unit vectors of AW polarizations. The quantity

$$N_{il} = C_{ijkl}m_j m_k \qquad (11)$$

in Eq. (10) represents a second-rank Christoffel tensor. We note that the AW velocities calculated for the BK7 glass are equal to $v_{33} = 6048$ m/s and $v_{31} = v_{32} = 3680$ m/s .

The changes in the elastic stiffnesses (or the AW velocities) occurring under mechanical stress (or strain) are known as an acousto-elastic effect [2, 3]. They are described by the relation

$$\Delta C_{ijkl} = \theta_{ijklmn}e_{mn} = \theta_{ijklmn}S_{nmrt}\sigma_{rt} = \Theta_{ijklrt}\sigma_{rt} , \qquad (12)$$

where ΔC_{ijkl} denotes the increment of elastic stiffness, θ_{ijklmn} and Θ_{ijklmn} are the sixth-rank polar tensors with the internal symmetry $[[V^2]^2][V^2]$, e_{mn} and σ_{rt} imply respectively the strain and stress tensors, and S_{nmrt} is the tensor of elastic compliances. Notice that the acousto-elastic effect is an analogue of elasto-optic (or piezo-optic) effect in optics, whereas the changes in the AW velocities induced by the stresses 10^6 N/m^2 are usually small enough (e.g., ~ 10 m/s –see Ref. [2]).

The numerical values of the Θ_{ijklrt} components for the BK7 glass are not available in the literature. In our simulations, we have taken the Θ_{ijklrt} values that follow from the experimental data for the AW-velocity changes observed in rocks [2]. As a result, we arrive at $\Theta_{111} = 100$, $\Theta_{121} = 200$, $\Theta_{221} = 600$, $\Theta_{231} = 400$ and $\Theta_{134} = 560$. The following relationships among the tensor components are valid for the isotropic media [14]:

$$\Theta_{564} = \frac{1}{8}(\Theta_{111} - 2\Theta_{121} - \Theta_{221} + 2\Theta_{231}), \quad \Theta_{441} = \frac{1}{2}(\Theta_{121} - \Theta_{231}), \quad \Theta_{551} = \frac{1}{4}(\Theta_{111} - \Theta_{221}). \quad (13)$$

Thus, the Christoffel tensor components are given by $N_{11} = 0.5(C_{11} - C_{12}) + \Theta_{441}\sigma_2(X,Y)$, $N_{22} = 0.5(C_{11} - C_{12}) + \Theta_{551}\sigma_2(X,Y)$, $N_{33} = C_{11} + \Theta_{221}\sigma_2(X,Y)$, $N_{23} = N_{13} = 0$ and $N_{12} = \Theta_{564}\sigma_6(X,Y)$. Then the AW velocities under the bending stresses can be represented as

$$v_{32} = \left(\frac{(C_{11} - C_{12}) + (\Theta_{441} + \Theta_{551})\sigma_2(X,Y) - \sqrt{(\Theta_{441} - \Theta_{551})^2\sigma_2^2(X,Y) + 4\Theta_{564}^2\sigma_6^2(X,Y)}}{2\rho} \right)^{\frac{1}{2}} , \quad (14)$$

$$v_{31} = \left(\frac{(C_{11} - C_{12}) + (\Theta_{441} + \Theta_{551})\sigma_2(X,Y) + \sqrt{(\Theta_{441} - \Theta_{551})^2\sigma_2^2(X,Y) + 4\Theta_{564}^2\sigma_6^2(X,Y)}}{2\rho} \right)^{\frac{1}{2}} , \quad (15)$$

$$v_{33} = \left(\frac{1}{\rho}(C_{11} + \Theta_{221}\sigma_2(X,Y)) \right)^{\frac{1}{2}} . \qquad (16)$$

It is seen that the AW velocities v_{32} and v_{31} become different under the bending stress. Then we obtain

$$v_{31}^2 - v_{32}^2 = \frac{1}{\rho}\sqrt{(\Theta_{441} - \Theta_{551})^2\sigma_2^2(X,Y) + 4\Theta_{564}^2\sigma_6^2(X,Y)} , \qquad (17)$$

and

$$\Delta v = v_{31} - v_{32} \simeq \frac{1}{2}\sqrt{\frac{(\Theta_{441} - \Theta_{551})^2\sigma_2^2(X,Y) + 4\Theta_{564}^2\sigma_6^2(X,Y)}{2\rho(C_{11} - C_{12})}} . \qquad (18)$$

Finally, this yields in

Ukr. J. Phys. Opt. 2022, Volume 23, Issue 3

169

$$\Delta v \simeq \frac{3P_1}{2bh^3d} \Theta_{564} \sqrt{\frac{\frac{1}{16}\left(d(2l-d)-4Y^2\right)^2 X^2 + \left(\frac{h^2}{4}-X^2\right)^2 Y^2}{\rho(C_{11}-C_{12})}} . \qquad (19)$$

Under condition $r \rightarrow 0$, the orientation angle of the eigenvectors of the Christoffel tensor with respect to the X axis is given by the formula

$$\tan 2\zeta_Z^a = -\frac{\sigma_6}{\sigma_2} = \frac{h^2}{d(2l-d)}\tan\varphi . \qquad (20)$$

It is evident that the dependence of ζ_Z^a on the azimuthal angle φ corresponds to the anisotropic vortex appearing due to a mixed screw-edge dislocation of the phase front. Under the condition $h^2/d_a(2l-d_a)=1$ (or $d_a = l - \sqrt{l^2-h^2} \simeq h^2/2l$ at $h^2 \ll l^2$), Eq. (20) can be reduced to

$$\tan 2\zeta_Z^a = \tan\varphi \ \ (\text{or } \zeta_Z^a = \varphi/2), \qquad (21)$$

where d_a is the distance on which the mechanical stress must be distributed in order to generate a purely screw acoustic dislocation. Then Eq. (19) can be rewritten in the form

$$\Delta v \simeq \frac{3P_1 h}{4bh^3 d_a} \Theta_{564} \sqrt{\frac{X^2+Y^2}{\rho(C_{11}-C_{12})}} . \qquad (22)$$

Eq. (21) describes a topological defect of orientation of the eigenvectors of the Christoffel tensor with the strength equal to $q = \frac{1}{2}$ and Eq. (22) implies a conical distribution of the difference of phase velocities of the AWs. Finally, it is obvious from Eqs. (6)–(8) and Eqs. (20)–(22) that the conditions for generating the isotropic optical and acoustic vortices are different.

3. Results and discussion

In case of our particular geometry described above, the isotropic optical vortex should correspond to the parameter $d_o = 0.66$ mm [5]. The calculated dependences of the rotation angle of optical indicatrix and the orientation angle of eigenvectors of the Christoffel tensor are shown in Fig. 2. The angle of optical-indicatrix rotation depends linearly on the azimuthal angle and the orientation angle of the eigenvectors of the Christoffel tensor oscillates with changing φ. The dependence of the difference of AW velocities on the X and Y coordinates represents a conical surface with a non-circular cross-section (see Fig. 3a, b), while its optical analogue is a conical surface with the axis of revolution parallel to the Z axis (see Fig. 3c, d). Then the optical-polarization singularity would produce an isotropic singly charged optical vortex nested in the emergent optical beam, while the AW propagating inside the sample would bear an anisotropic singly charged acoustic vortex.
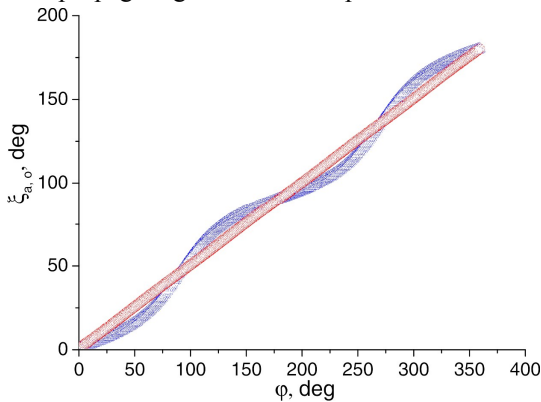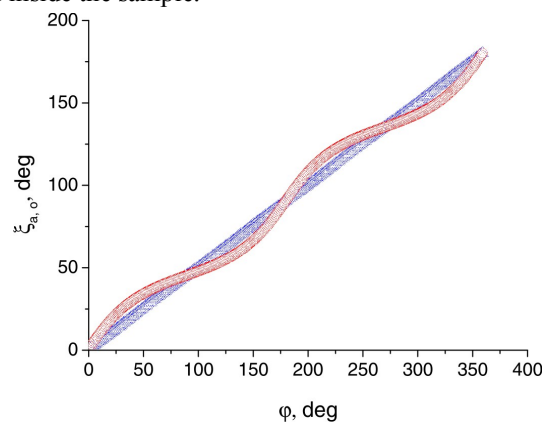

Fig. 2. Dependences of rotation angle of optical indicatrix (circles) and eigenvectors of Cristoffel tensor (triangles) on the azimuthal angle φ, as calculated at $d = 0.66$ mm.
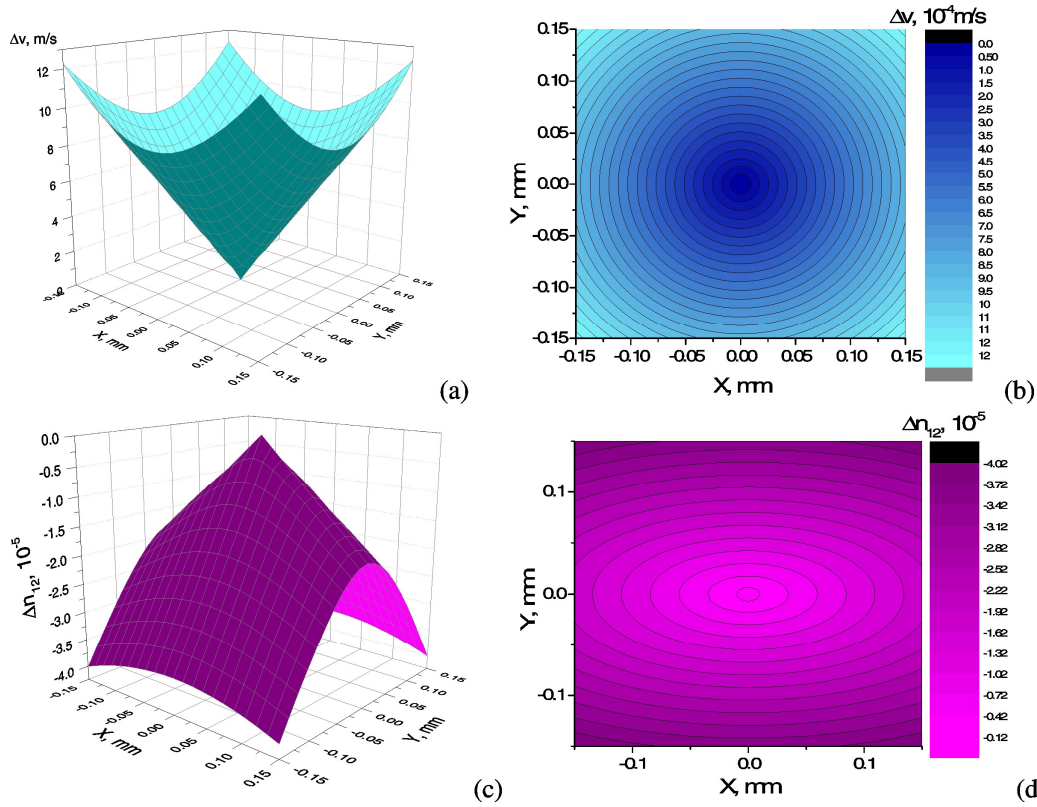
170

Ukr. J. Phys. Opt. 2022, Volume 23, Issue 3
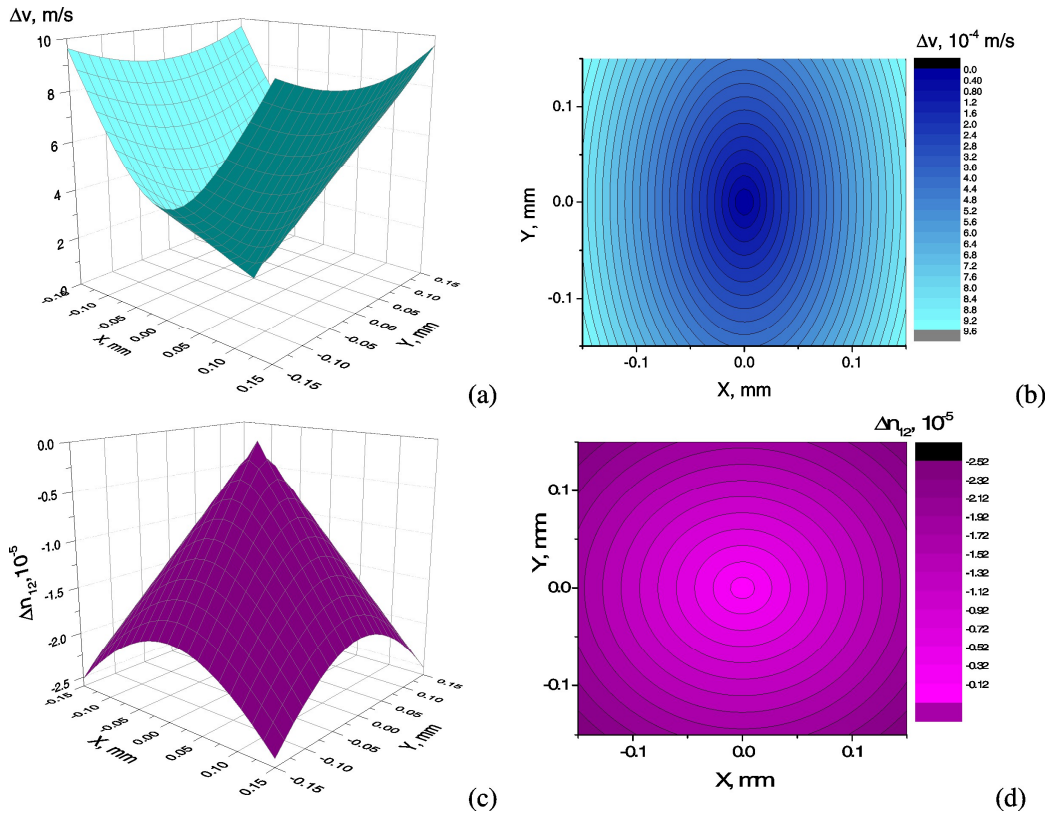
Fig. 3. Spatial distributions of difference of the AW velocities (panel a) and optical birefringence (panel c), and their projections on the *XY* plane (panels b and d, respectively), as calculated at *d* = 0.66 mm.

The opposite situation is observed at d_a = 0.33 mm. Then the dependence of the orientation angle of eigenvectors of the Christoffel tensor on the azimuthal angle is linear, contrary to the dependence of orientation angle of the optical indicatrix (see Fig. 4). The appropriate dependences of the optical birefringence and the difference of AW velocities on the *X* and *Y* coordinates are presented in Fig. 5, together with their projections on the *XY* plane. The behaviour described above would mean appearance of an anisotropic optical vortex behind the sample and an isotropic singly charged acoustic vortex inside the sample.

Fig. 4. Dependences of rotation angle of optical indicatrix (circles) and eigenvectors of Cristoffel tensor (triangles) on the azimuthal angle φ, as calculated at *d* = 0.33 mm.

Ukr. J. Phys. Opt. 2022, Volume 23, Issue 3

171

Fig. 5. Spatial distributions of difference of the AW velocities (panel a) and optical birefringence (panel c), and their projections on the *XY* plane (panels b and d, respectively), as calculated at *d* = 0.33 mm.

The projections displayed in Fig. 3b and Fig. 5d are six-order geometric figures rather than ellipses (see Eqs. (5) and (19)). In order to know at which *d* values these figures are characterized by the unit ratio of semi-axes, one can plot the dependences of the acoustic and optical anisotropy parameters $\chi_a = \dfrac{h^2}{d(2l-d)}$ and $\chi_o = \dfrac{2h^2}{d(2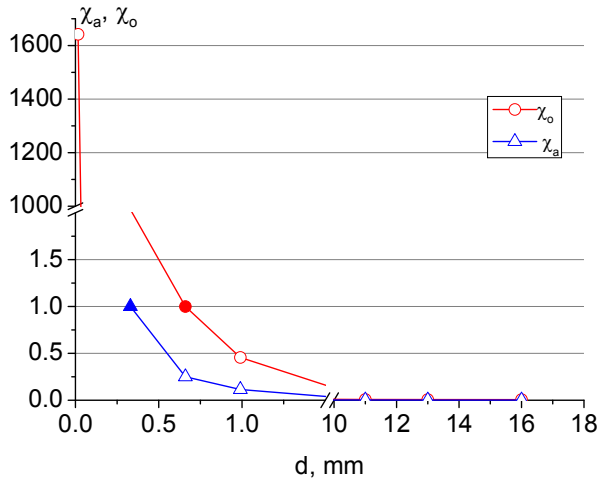l-d)}$ on the distance *d* over which the mechanical load is distributed. For this aim, let us rewrite Eqs. (5) and (19) with neglecting higher-order *r* terms under assumption of $r \to 0$. Then Eqs. (5) and (19) would read respectively as

$$
\begin{aligned}
\Delta n_{12} &= \frac{3n^3 P_1}{bh^3 d}\pi_{66}\sqrt{\frac{d^2(2l-d)^2}{16}r^2\cos^2\varphi + \frac{h^4}{4}r^2\sin^2\varphi} \\
&= \frac{3n^3 P_1}{2bh^3 d}\pi_{66}\sqrt{\frac{d^2(2l-d)^2}{4}X^2 + h^4 Y^2}
\end{aligned}
\tag{23}
$$

$$
\begin{aligned}
\Delta v &= \frac{3P_1}{2bh^3 d\left(\rho(C_{11}-C_{12})\right)^{1/2}}\Theta_{564}\sqrt{\frac{d^2(2l-d)^2}{16}r^2\cos^2\varphi + \frac{h^4}{16}r^2\sin^2\varphi} \\
&= \frac{3P_1}{8bh^3 d\left(\rho(C_{11}-C_{12})\right)^{1/2}}\Theta_{564}\sqrt{d^2(2l-d)^2 X^2 + h^4 Y^2}
\end{aligned}
\tag{24}
$$

It is evident that the both relations describe ellipses. Fig. 6 shows the dependences of

anisotropy parameters χ_a and χ_o on the load-distribution distance d. It is obvious that χ_a and χ_o are equal to unity at some specific (though different) d values: we have $\chi_a = 1$ at $d_a = 0.33$ mm and $\chi_o = 1$ at $d_o = 0.66$ mm.

Fig. 6. Dependences of anisotropy parameters χ_a and χ_o on the distance d over which mechanical load is distributed.

Now let us consider a backward collinear AO diffraction of the incident optical wave by the AW. For the case of AO interaction in the glass-like media, the collinear diffraction cannot be implemented since the appropriate elasto-optic coefficients (p_{14}, p_{24}, p_{15}, p_{25}, p_{64} and p_{65}) are equal to zero. However, these coefficients remain nonzero in the crystals belonging to the point symmetry group 3m (e.g., LiNbO$_3$) or the other symmetry groups that contain the three-fold axes among their symmetry operations. Note that Eqs. (6) and (20) (as well as Eqs. (23) and (24)) derived above for the isotropic glass media remain almost the same for the crystals of the symmetry group 3m. Namely, we have

$$
\tan 2\zeta_Z^o = -\frac{2\sigma_6}{\sigma_2} = \frac{2h^2}{d(2l-d)}\tan\varphi,
$$
$$
\tan 2\zeta_Z^a = -\frac{\sigma_6}{\sigma_2} = \frac{h^2}{d(2l-d)}\tan\varphi,
\tag{25}
$$

$$
\Delta n_{12} = \frac{3n_o^3 P_1}{2bh^3 d}\pi_{66}\sqrt{\frac{d^2(2l-d)^2}{4}X^2 + h^4 Y^2},
$$
$$
\Delta v = \frac{3P_1(\Theta_{441}-\Theta_{551})}{2bh^3 d\left(\rho C_{44}\right)^{1/2}}\sqrt{d^2(2l-d)^2 X^2 + h^4 Y^2},
\tag{26}
$$

where n_o is the ordinary refractive index. The only differences are the effective piezo-elastic coefficient $\Theta_{441} - \Theta_{551}$ and the elastic stiffness C_{44}, which replace the coefficients Θ_{564} and $C_{11} - C_{12}$ for glasses.

Notice also that, contrary to the case of mechanical torsion [1], bending can produce anisotropic optical and acoustic vortices. This anisotropy manifests itself as a non-monotonic change in the phase under helicoidal rotation around the vortex core. The dependences of orientations of the optical indicatrix and the Christoffel eigenvectors on the azimuthal angle are defined by the relations

$$
\zeta_Z^o = \frac{1}{2}\arctan\left(\chi_o \tan\varphi\right), \quad \zeta_Z^a = \frac{1}{2}\arctan\left(\chi_a \tan\varphi\right),
\tag{27}
$$

Imagine that a right-handed (RH) circular acoustic Gaussian beam is excited in a crystal and propagates along the Z axis. Then the corresponding displacement vector can be written as

$$u^{RH} = u_0 \begin{bmatrix} 1 \\ i \end{bmatrix} e^{-iK_{ac}Z}, \tag{28}$$

where Ω and K_{ac} are respectively the frequency and the wavevector of AW, and u_0 is the unit amplitude of displacement vector. This wave is characterized by the spin angular momentum equal to $\hbar$. When the bending stress is applied (see Fig. 1), the AW velocities v_{31} and v_{32} become different and a topological defect of the eigenvectors of the Christoffel tensor with the strength $q = \frac{1}{2}$ appears. Then the initial RH-polarized acoustic Gaussian beam can be decomposed into the RH-polarized Gaussian beam and the left-handed (LH) beam bearing the acoustic vortex. This process can be described as (see Ref. [1])

$$u^{out}(r, \varphi) = u_0 \cos \frac{\Delta\Gamma_{ac}(r, P_1)}{2} \begin{bmatrix} 1 \\ i \end{bmatrix} e^{-iK_{ac}Z}$$
$$+ iu_0 \sin \frac{\Delta\Gamma_{ac}(r, P_1)}{2} \begin{bmatrix} 1 \\ -i \end{bmatrix} e^{i \arctan(\chi_a \tan\varphi) - iK_{ac}Z} . \tag{29}$$

Here $\Delta\Gamma_{ac}(r, P_1) = \left(\dfrac{\Omega}{v_{31}(r, P_1)} - \dfrac{\Omega}{v_{32}(r, P_1)} \right) b$ is the phase difference between the transverse AWs which have their polarizations orthogonal (i.e., parallel to the X and Y axes) and propagate with the velocities $v_{31}(r, P_1)$ and $v_{32}(r, P_1)$, and $u^{out}(r, \varphi)$ denotes the output-AW displacement vector.

As seen from Eq. (29), the phase of the outgoing AW depends nonlinearly upon the azimuthal angle. Seemingly, this should lead to dependence of the vortex charge on the angle φ (i.e., $l = \dfrac{1}{\varphi} \arctan(\chi_a \tan\varphi)$). However, such a dependence rather means that the phase change has an oscillating character (i.e., it accelerates and slowdowns periodically), while the phase change is equal to 2π within the period of AW. Therefore χ_a and χ_o represent morphological parameters of the vortices, which define their internal structure. Hence, an anisotropic vortex with the charge $l = 2q = 1$ is generated. Moreover, Eq. (29) describes conversion of the spin angular momentum to the OAM, since the second term in the right-hand side of Eq. (29) corresponds to the AW with the helicoidal phase front and the LH polarization (i.e., the spin angular momentum equal to $-\hbar$ and the OAM equal to $\hbar$).
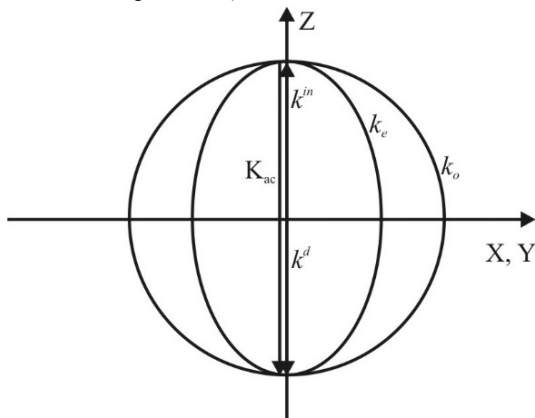
Fig. 7. Schematic view of phase-matching conditions provided at a backward collinear diffraction: k^{in} and k^d are wavevectors of the incident and diffracted optical waves, K_{ac} is wavevector of the AW, and k_o and k_e denote respectively wavevectors of the ordinary and extraordinary optical waves (a LiNbO$_3$ crystal is taken as an example).

Now let us consider a particular case of backward collinear AO diffraction illustrated in Fig. 7. A linearly polarized incident optical wave with its polarization parallel to the X (or Y) axis is described by the state vectors

$$D_1^{in} = D_o \begin{pmatrix} 1 \\ 0 \end{pmatrix} e^{-ik_{in}Z} \text{ or } D_2^{in} = D_o \begin{pmatrix} 0 \\ 1 \end{pmatrix} e^{-ik_{in}Z} . \tag{30}$$

As a result of bending-induced singularity, we arrive at the Jones matrix [15]

$$M(X,Y) = \cos\frac{\Delta\Gamma_o(r,P_1)}{2}\begin{bmatrix} 1 & 0 \\ 0 & 1 \end{bmatrix} + i\sin\frac{\Delta\Gamma_o(r,P_1)}{2}\begin{bmatrix} \cos 2\zeta_Z^o & \sin 2\zeta_Z^o \\ \sin 2\zeta_Z^o & -\cos 2\zeta_Z^o \end{bmatrix}, \tag{31}$$

where $\Delta\Gamma_o(r,P_1) = \frac{2\pi}{\lambda}\Delta n_{12} b$ is the bending-induced optical phase difference and D_0 the unit electric-induction amplitude. The X- or Y-polarized incident optical waves are decomposed inside the crystal:

$$D(X,Y) = D_0 \cos\frac{\Delta\Gamma_o(r,P_1)}{2}\begin{bmatrix} 1 \\ 0 \end{bmatrix}e^{-ik_{in}Z} + iD_0\sin\frac{\Delta\Gamma_o(r,P_1)}{2}\begin{bmatrix} \cos 2\zeta_Z^o \\ \sin 2\zeta_Z^o \end{bmatrix}e^{-ik_{in}Z}, \tag{32}$$

$$D(X,Y) = D_0 \cos\frac{\Delta\Gamma_o(r,P_1)}{2}\begin{bmatrix} 0 \\ 1 \end{bmatrix}e^{-ik_{in}Z} + iD_0\sin\frac{\Delta\Gamma_o(r,P_1)}{2}\begin{bmatrix} \sin 2\zeta_Z^o \\ -\cos 2\zeta_Z^o \end{bmatrix}e^{-ik_{in}Z}. \tag{33}$$

Notice that Eqs. (32) and (33) contain the two terms. The first term describes the wave with the incident polarization and the second one corresponds to the optical vector beam with the unit polarization order. In general, this vector beam is close to the elliptical one [16]. Following from Eq. (29), the displacement vector of the AW bearing the vortex is given by the relation

$$u^{LH} = u_0 \sin\frac{\Delta\Gamma_{ac}(r,P_1)}{2}\begin{bmatrix} 1 \\ -i \end{bmatrix}e^{i\arctan(\chi_a\tan\varphi)-iK_{ac}Z}. \tag{34}$$

The strain-tensor components caused by this AW read as

$$e_4 = 2e_{23} = \left(\frac{\partial u_2}{\partial Z} + \frac{\partial u_3}{\partial Y}\right) = -K_{ac}e_0\sin\frac{\Delta\Gamma_{ac}(r,P_1)}{2}e^{i\arctan(\chi_a\tan\varphi)-iK_{ac}Z},$$
$$e_5 = 2e_{13} = \left(\frac{\partial u_1}{\partial Z} + \frac{\partial u_3}{\partial X}\right) = -iK_{ac}e_0\sin\frac{\Delta\Gamma_{ac}(r,P_1)}{2}e^{i\arctan(\chi_a\tan\varphi)-iK_{ac}Z}, \tag{35}$$

with e_0 being the unit strain. Then the electric-field components of the diffracted wave for the cases of X- and Y-polarized incident optical waves can be written respectively as

$$E^d = -ip_{14}\sin\frac{\Delta\Gamma_o(r,P_1)}{2}\sin\frac{\Delta\Gamma_{ac}(r,P_1)}{2}\begin{bmatrix} 1 \\ i \end{bmatrix}e^{i\left[\arctan(\chi_o\tan\varphi)+\arctan(\chi_a\tan\varphi)-(k^{in}+K_{ac})Z\right]} \tag{36}$$

and

$$E^d = -p_{14}\sin\frac{\Delta\Gamma_o(r,P_1)}{2}\sin\frac{\Delta\Gamma_{ac}(r,P_1)}{2}\begin{bmatrix} 1 \\ i \end{bmatrix}e^{i\left[\arctan(\chi_o\tan\varphi)+\arctan(\chi_a\tan\varphi)-(k^{in}+K_{ac})Z\right]}, \tag{37}$$

with p_{14} being the elasto-optic coefficient. Note that D_0, e_0 and the corresponding unit parameter referred to K_{ac} are not written down in Eqs. (36) and (37) for the reasons of brevity.

One can see that the electric fields of the diffracted optical waves correspond to the RH-polarized waves containing a topological defect of their phase fronts. Its strength is given by a sum of the strengths of defects referred to the optical wave and the AW, which involves the both anisotropy parameters: $q = \frac{1}{2}\left(\arctan(\chi_o\tan\varphi) + \arctan(\chi_a\tan\varphi)\right)$. In other words, these waves bear a doubly

charged optical vortex with the OAM equal to $l = \dfrac{1}{\varphi}\left(\arctan\left(\chi_o \tan\varphi \right) + \arctan\left(\chi_a \tan\varphi \right) \right)$. Fig. 8 displays dependences of the phase of this vortex, $\delta = \arctan(\chi_o \tan\varphi) + \arctan(\chi_a \tan\varphi)$, on the azimuthal angle φ, as calculated at different anisotropic parameters χ_o and χ_a. Each dependence corresponds to some distance d taken from Fig. 6.
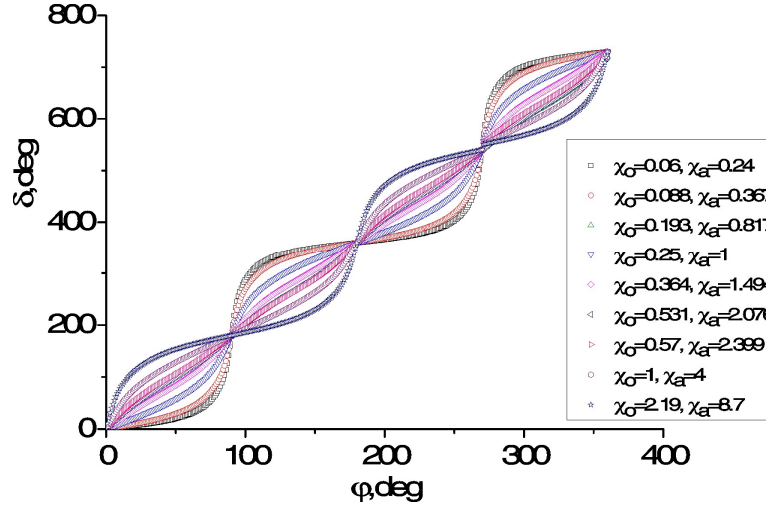
Fig. 8. Dependences of phase δ of the vortex on the azimuthal angle φ, as calculated at different anisotropic parameters χ_o and χ_a.

Since the phase is changed by 4π at the azimuthal change of 2π (see Fig. 8), the diffracted optical wave bears a doubly charged optical vortex and the strength of topological defects embedded in the acoustic and optical beams are summed up. It is also noteworthy that the dependences of the phase on the angle φ are nonlinear and have a step-like character. This means that the optical vortex is anisotropic. The dependence of the phase on the angle φ acquires a linear character at some specific values of the anisotropic parameters (e.g., $\chi_o \approx 0.531$ and $\chi_a \approx 2.076$ at $d = 0.47$ mm). Then the vortex nested in the diffracted optical beam becomes isotropic. Notice that, in our recent work [1], we have not considered a vector character of the optical beam appearing under condition of linearly polarized incident optical beam. This has resulted in an error corrected later in Ref. [4].

If the incident AW is LH-polarized, it excites the acoustic vortex wave with the RH polarization and the OAM $l = -\hbar$. In the case of AO interaction of the optical wave described by Eqs. (30), (32) and (33) with this AW, the diffracted optical wave represents a circular wave with the LH polarization and the OAM equal to $l = -2\hbar$.

In the case of AO interaction involving the RH-polarized incident optical wave,

$$D^{RH} = D_0 \begin{bmatrix} 1 \\ i \end{bmatrix} e^{-ik^{in}Z}, \tag{38}$$

and the LH-polarized AW (see Eqs. (34) and (35)), the electric induction of the optical wave inside the crystal can be described by the sum of two terms:

$$D(r,\varphi) = D_0 \cos\frac{\Delta\Gamma_o\left(r,P_1\right)}{2}\begin{bmatrix} 1 \\ i \end{bmatrix} e^{-ik^{in}Z} + iD_0 \sin\frac{\Delta\Gamma_o\left(r,P_1\right)}{2}\begin{bmatrix} 1 \\ -i \end{bmatrix} e^{i\arctan\left(\chi_o \tan\varphi\right)-ik^{in}Z}. \tag{39}$$

The second term in the right-hand side of Eq. (39) represents the LH-polarized wave that bears a singly charged vortex. Then the electric field of the diffracted wave can be written as

$$E^d = -2ip_{14}\sin\frac{\Delta\Gamma_{ac}\left(r,P_1\right)}{2}\sin\frac{\Delta\Gamma_o\left(r,P_1\right)}{2}\begin{bmatrix}1\\i\end{bmatrix}e^{i\left(\arctan\left(\chi_a\tan\varphi\right)+\arctan\left(\chi_o\tan\varphi\right)\right)-i(k^{in}+K_{ac})Z}, \quad (40)$$

As seen from Eq. (40), the RH-polarized diffracted optical wave bears a doubly charged anisotropic vortex.

In case when the incident optical wave is RH-polarized (and the excited AW is LH-polarized), the topological defects embedded in the incident acoustic and optical beams would annihilate and the diffracted optical wave becomes vortex-free. Then the phase is given by the relation $\delta = \arctan(\chi_o\tan\varphi) - \arctan(\chi_a\tan\varphi)$. The dependences of the phase of this wave on the azimuthal angle φ calculated at different anisotropic parameters χ_o and χ_a are illustrated in Fig. 9. One can see that the phase oscillates around a zero value and the phase increment is equal to zero when the azimuthal angle changes by 2π. In general, these oscillations are not harmonic. It is only at the anisotropy parameters $\chi_o \approx 0.531$ and $\chi_a \approx 2.076$ (taken at $d = 0.47$ mm) that the dependence of the phase on the angle φ becomes sinusoidal. Note also that the dependences of the phase on the azimuthal angle presented in Fig. 9 do not correspond to the screw dislocation of the phase front. They are close to the two edge dislocations crossed at the right angle.
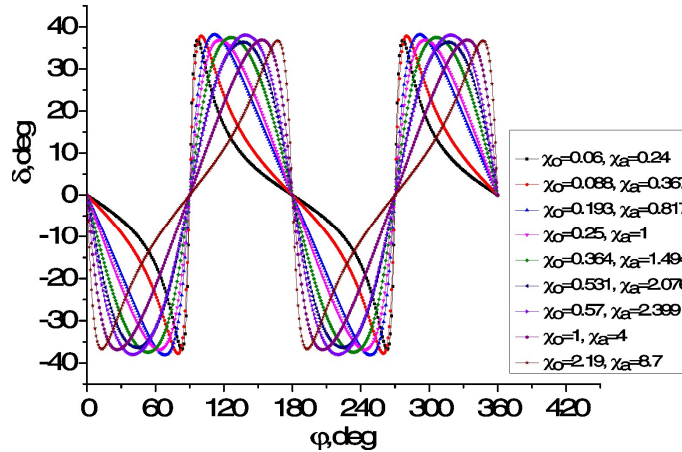
Fig. 9. Dependences of phase δ of the diffracted wave (see Eq. (40)) on the azimuthal angle φ, as calculated at different anisotropic parameters χ_o and χ_a.

4. Conclusions

In the present work, we have shown that the bending mechanical stresses can generate the polarization singularity for transverse acoustic waves (i.e., the topological defect of eigenvectors of the Christoffel tensor with the strength equal to ½). In its turn, this results in induction of the singly charged acoustic vortices. The properties of such vortices have been analyzed. In particular, we have demonstrated that, in general, they are anisotropic. Nonetheless, the vortices can be transformed into isotropic ones at some specific geometrical parameters of distributed mechanical loading. It is very important that the acoustic vortices generated through the bending stresses can be produced even in isotropic solid-state media.

The process of collinear backward AO diffraction has been considered for the case of interaction of optical waves with the AWs that bear bending-generated topological defects of the

Ukr. J. Phys. Opt. 2022, Volume 23, Issue 3

177

phase front. This has been done on a specific example of crystals belonging to the point symmetry group 3m. We have shown that the vector beam with the unit polarization order is generated in the crystals in case of the linearly polarized incident optical beam. The AO interaction of this vector beam with the acoustic beam bearing the singly charged anisotropic vortex produces the diffracted optical wave which is also vortex-bearing. The embedded topological defect of the phase front of this wave has the strength given by the sum of the strengths of topological defects of the incident optical wave and the AW. Then the diffracted optical beam represents the anisotropic vortex beam with the OAM equal to $2\hbar$.

When both the incident optical wave and the AW nest bending-induced singly charged anisotropic vortices, the diffracted optical wave would also bear the vortex. Its charge is given by a linear combination that involves the charges corresponding to the AW and the incident optical waves and the parameters of acoustic and optical anisotropies. When the signs of the OAMs of the interacting AW and the optical wave are the same, the diffracted optical wave bears the doubly charged anisotropic optical vortex. It can be transformed into the isotropic vortex at a specific balance of anisotropy parameters. Finally, when the signs of the OAMs are opposite, the topological defects embedded in the interacting waves annihilate and the diffracted optical wave becomes vortex-free.

Acknowledgement

References

1. Mys O, Kostyrko M, Adamenko D, Skab I and Vlokh R, 2022. Acoustic polarization singularities arising under torsion and orbital angular momentum exchange at the backward collinear acousto-optic diffraction: a case of crystals with point symmetry 3m. Ukr. J. Phys. Opt. **23**: 107–115.

2. Huang Xiaojun, Burns D R and Toksoz M N, 2001. The effect of stresses on the sound velocity in rocks: theory of acoustoelasticity and experimental measurements. Massachusetts Institute of Technology. Earth Resources Laboratory. URL: http://hdl.handle.net/1721.1/68599

3. Hmiel A, Winey J M, Gupta Y M and Desjarlais M P, 2016. Nonlinear elastic response of strong solids: first-principles calculations of the third-order elastic constants of diamond. Phys. Rev. B. **93**: 174113.

4. Mys O, Kostyrko M, Adamenko D, Skab I and Vlokh R, 2022. Acoustic polarization singularities arising under torsion and orbital angular momentum exchange at the backward collinear acousto-optic diffraction: a case of crystals with point symmetry 3m. Errata. Ukr. J. Phys. Opt. **23**: 150–154.

5. Skab I, Vasylkiv Y and Vlokh R, 2012. Induction of optical vortex in the crystals subjected to bending stresses. Appl. Opt. **51**: 5797–5805.

6. Guang-Hoon Kim, Hae June Lee, Jong-Uk Kim and Hyyong Suk, 2003. Propagation dynamics of optical vortices with anisotropic phase profiles. J. Opt. Soc. Amer. B. **20**: 351–359.

7. Molina-Terriza G, Recolons J, Torres J P and Torner L, 2001. Observation of the dynamical inversion of the topological charge of an optical vortex. Phys. Rev. Lett. **87**: 023902.

8. https://www.pgo-online.com/intl/BK7.html

9. Krupych O, Savaryn V, Skab I and Vlokh R, 2011. Interferometric measurements of piezooptic coefficients by means of four-point bending method. Ukr. J. Phys. Opt. **12**: 150–159.

10. Timoshenko S P. Strength of Materials. Part I: Elementary Theory and Problems. Moscow: Nauka, 1965.
11. Timoshenko S P. Strength of materials. Part II: Advanced Theory and Problems. Moscow: Nauka, 1965.
12. Lamaitre G R. Astronomical Optics and Elasticity Theory. Berlin Heidelberg: Springer-Verlag, 2009.
13. https://www.pgo-online.com/intl/BK7.html
14. Sirotin Yu I and Shaskolskaya M P. Fundamentals of Crystal Physics. Moscow: Mir Publishers, 1982.
15. Marrucci L, 2008. Generation of helical modes of light by spin-to-orbital angular momentum conversion in inhomogeneous liquid crystals. Mol. Cryst. Liq. Cryst. **488**: 148–162.
16. Yue Pan, Yongnan Li, Si-Min Li, Zhi-Cheng Ren, Ling-Jun Kong, Chenghou Tu and Hui-Tian Wang, 2014. Elliptic-symmetry vector optical fields. Opt. Express. **22**: 19302−19313.

Анотація. *Показано, що механічне напруження згину може спричинити появу топологічного дефекту орієнтації власних векторів тензора Крістофеля з силою ½. Це означає генерацію однозарядного акустичного вихору для поперечних акустичних хвиль. Загалом цей вихор є анізотропним, хоча при деяких геометричних параметрах розподіленого механічного навантаження він може трансформуватися в ізотропний. Акустичні вихори, породжені внаслідок дії напружень згину, можуть формуватися навіть в ізотропних твердотільних середовищах. На прикладі кристалів, що належать до групи точкової симетрії 3т, ми також розглянули процес зворотної колінеарної акустооптичної дифракції для випадку взаємодії оптичних та акустичних хвиль, які несуть генеровані згином топологічні дефекти їхніх фазових фронтів. Показано, що у випадку падаючої оптичної хвилі з лінійною поляризацією в кристалах генерується векторний пучок з одиничним порядком поляризації. Акустооптична взаємодія цього векторного пучка з акустичним пучком, який несе однозарядний анізотропний вихор, породжує дифраговану оптичну хвилю, яка також несе вихор. Вбудований топологічний дефект фазового фронту, пов'язаний з цим вихором, має силу, яка визначається сумою сил топологічних дефектів падаючої оптичної хвилі та акустичної хвилі. Дифрагований оптичний пучок є анізотропним вихровим пучком із орбітальним кутовим моментом (ОКМ), що дорівнює 2ħ. Коли і акустична хвиля, і падаюча оптична хвиля містять індуковані згином однозарядні анізотропні вихри, дифрагована оптична хвиля також несе вихор. Його заряд є лінійною комбінацією зарядів, пов'язаних із акустичною та падаючою оптичною хвилями, яка включає параметри акустичної та оптичної анізотропії. Якщо знаки ОКМ взаємодіючих акустичної та оптичної хвиль однакові, то дифрагована оптична хвиля несе подвійно заряджений анізотропний оптичний вихор. При деяких специфічних параметрах анізотропії він може бути перетворений на ізотропний вихор. Нарешті, топологічні дефекти, закладені у взаємодіючі хвилі, анігілюють, а дифрагована оптична хвиля стає безвихровою, якщо знаки ОКМ взаємодіючих хвиль протилежні.*